

ChemComm

Accepted Manuscript



This is an *Accepted Manuscript*, which has been through the Royal Society of Chemistry peer review process and has been accepted for publication.

Accepted Manuscripts are published online shortly after acceptance, before technical editing, formatting and proof reading. Using this free service, authors can make their results available to the community, in citable form, before we publish the edited article. We will replace this *Accepted Manuscript* with the edited and formatted *Advance Article* as soon as it is available.

You can find more information about *Accepted Manuscripts* in the [Information for Authors](#).

Please note that technical editing may introduce minor changes to the text and/or graphics, which may alter content. The journal's standard [Terms & Conditions](#) and the [Ethical guidelines](#) still apply. In no event shall the Royal Society of Chemistry be held responsible for any errors or omissions in this *Accepted Manuscript* or any consequences arising from the use of any information it contains.



Journal Name

COMMUNICATION

Facile method for fabrication of buckled PDMS silver nanorod arrays as active 3D SERS cage for bacterial sensing†

Received 00th January 20xx,
Accepted 00th January 20xx

Samir Kumar,^a Devesh K. Lodhi,^a Pratibha Goel,^a Neeti,^b Prashant Mishra,^b and, J. P. Singh*

DOI: 10.1039/x0xx00000x

www.rsc.org/

Our results demonstrate that it is possible, by means of generation of buckles on the silver nanorod arrays (AgNRs) PDMS substrate to enhance the Raman signal of *P. aeruginosa* bacteria due to the formation of high density 'hot spots' among the AgNRs arrays which provides better entrapment and increases the net effective contact area of bacteria with the metal surface.

Pseudomonas aeruginosa is an opportunistic pathogen that colonizes on damage sites prone to infection such as burns, surgical wounds, respiratory tract and physically damaged eyes.^{1,2} *P. aeruginosa* also lead to serious pulmonary infections in cystic fibrosis and immunocompromised patients, mainly due to its high level of resistance to antibiotics. Successful antibiotic treatment of the infection relies on accurate and rapid identification of infectious pathogens. Conventional techniques used to identify bacteria includes biochemical tests such as Gram stain, enzyme activity tests and antibiotic susceptibility test.³ All these tests can be applied only on pure bacteria after incubating them in suitable growth medium.⁴ However, culturing bacteria is a time consuming procedure and cannot provide rapid identification and response.

Recently, surface enhanced Raman scattering (SERS) has emerged as a promising technique for chemical and biological sensing.^{5–8} There are many good works reported in the past several years for the bacteria measurement by SERS.^{9–11} SERS is a giant enhancement of Raman signal of a material in the vicinity of a rough metal surface.^{12,13} Special metallic protrusions and nanogaps serve as 'hot-spots' and can enhance the SERS signal by the electromagnetic coupling between the neighbouring nanoparticles. Rusciano et al. have used Raman spectroscopy to reveal bacteria in the sputa of patients with cystic fibrosis.¹⁴ Culture free diagnostic method based on SERS of pyocynin, a major biomarker of *P. aeruginosa* has been reported.¹⁵ However identifying appropriate

biomarker with high detection limit is a difficult task because of the limited literature on SERS detection of bacterial biomarkers.

SERS substrates have been fabricated ranging from rough metal surfaces to fractals, nanowires and well-ordered substrates.^{16–18} There are also few reports on the literatures on PDMS based SERS substrates.^{19–21} Although, SERS has emerged as a potential technique for chemical and biological sensing but it has few limitations like all the others techniques. One of the limitation of these SERS substrates lies in a fact that they are mostly two-dimensional (2D) planar systems. In 2D ordered substrates the number of hotspots is limited to only one Cartesian x-y plane. Whereas, three-dimensional (3D) cage-like structures can supply more hot spots which provide giant enhancement in Raman signal as compared to their 2D counterpart. 3D SERS active substrates have been fabricated by researchers using various methods such as e-beam lithography, reactive ion etching, template metal deposition and direct chemical methods.^{22–25} Recently, hierarchical 3D SERS substrate have been fabricated by integrating 3D photolithography microstructures and self-assembly of silver nanoparticles.^{26,27} However, the fabrication methods implied were complex, expensive and also technologically demanding for the large scale production.

We report a facile method to fabricate highly sensitive flexible Ag nanorod (AgNR) arrays based SERS substrates on buckled poly(dimethylsiloxane) (PDMS) for the detection of *P. aeruginosa*. The AgNRs were deposited on 30% pre-stretched PDMS using oblique angle deposition.^{28–30} Bacterial suspension (3 μ L, 108 cells/mL) was pipetted directly onto the AgNRs grown on stretched PDMS substrate. After performing SERS measurements on stretched AgNR-PDMS SERS substrate, the stress was released and SERS measurements were repeated. This AgNR-PDMS buckled system increases the number of hotspots and also provides the better entrapment of the bacteria *P. aeruginosa* onto the AgNRs giving rise to enhancement in the Raman signal. The buckled AgNR-PDMS arrays substrates exhibit about eleven-fold Raman signal enhancement compared to the pre-stretched AgNR-PDMS film. This excellent SERS enhancement may be attributed to the formation of

^aDepartment of Physics, Indian Institute of Technology Delhi, Hauz Khas, New Delhi 110016, India. E-mail: jpsingh@physics.iitd.ac.in

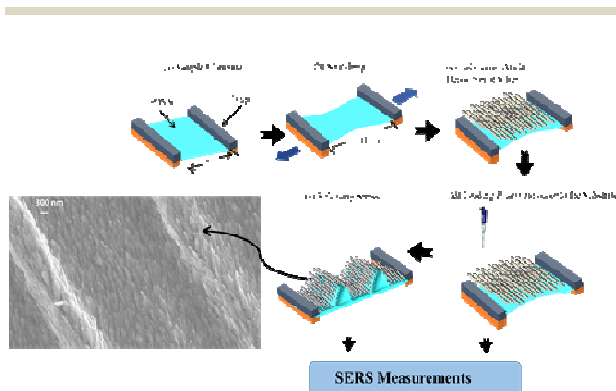
^bDepartment of Biochemical Engineering and Biotechnology, Indian Institute of Technology Delhi, Hauz Khas, New Delhi 110016, India.

†Electronic Supplementary Information (ESI) available: Experimental procedures and additional figures. See DOI: 10.1039/x0xx00000x

high density hot spots among the AgNRs and increase in the area for better interaction of bacteria with the metal surface which is supported by finite difference time domain (FDTD) simulations. These substrates can be a promising candidates for chemical and biological sensing applications.

The route followed for the fabrication of dual-scale roughened surface is schematically shown in Scheme 1. The average nanorod length and average inter-rod separation were found to be 1 μm and 130 nm, respectively. Without stretching, the primary surface consisting of nanoscale roughness due to AgNRs showed an isotropic and uniform density of AgNRs without any buckles or wrinkles. Whereas, for AgNRs deposited over pre-stretched elastomeric PDMS films subjected to initial mechanical strain (ϵ), upon releasing the strain, periodic wrinkles were formed to minimize the strain energy (Fig. S1, ESI[†]).

The SERS enhancement of an analyte mainly depends upon two factors (i) the proximity of the analyte group to the nanoscale metallic surface, and (ii) the density of the hot spots.¹³ The magnitude of SERS intensity decreases with increasing distance of the analyte from the active surface. The limited adhesion of the bacteria to the metallic surface/ hot spots limits the full potential of SERS for the diagnostic purposes. Due to the distance dependence the vibrational bands observed in the SERS enhancement mechanism of bacterial cells is dominated by the contributions from the cell wall components such as, lipids, lipopolysaccharides, or membrane protein of the outer cell layers.³¹ Figure 1 presents the Raman spectrum of *P. aeruginosa* measured on pre-stretched AgNR-PDMS substrate and after releasing the strain. The complex composition of the bacteria results into a complex Raman spectra. The detected main characteristic peaks of *P. aeruginosa* were at 730 cm^{-1} , 1010 cm^{-1} , 1323 cm^{-1} , and 1536 cm^{-1} .³² The Raman spectra of *P. aeruginosa* exhibited peaks from nucleic acids at 674 cm^{-1} , 730 cm^{-1} , and 1576 cm^{-1} ; from C-O-C at 1071 cm^{-1} ; from lipids at 1052 cm^{-1} and 1302 cm^{-1} ; and from proteins (amide III) between 1200-



Scheme 1. A schematic illustration of the fabrication of AgNRs-PDMS substrate. (a) The PDMS film was mounted on a custom-designed strain stage, (b) PDMS was stretched to a designated initial strain value (ϵ , defined as the ratio of increase in the film length (Δl) over its original length, l), (c) growth of Ag nanorods over pre-stretched PDMS film, (d) Loading *P. aeruginosa* onto the substrate and (e) releasing strain of the sample resulted into the formation of grooves as shown in magnified image.

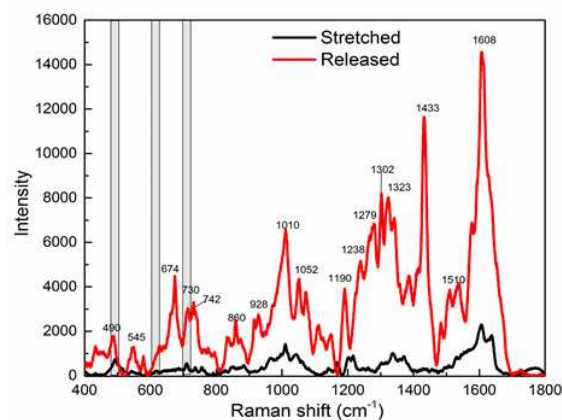


Figure 1. Raman spectra of *P. aeruginosa* on prestretched and relaxed AgNR-PDMS substrate. Readers may refer to ESI table T1 for Raman band assignments of *P. aeruginosa*. The shaded part corresponds to the peak due to PDMS, (Fig. S2, ESI[†]).

1400 cm^{-1} . The peaks at 1238- 1242 cm^{-1} , 1266- 1292 cm^{-1} and 1340- 1390 cm^{-1} are characteristic amino peaks.³³⁻³⁹

Fig. 1 clearly shows a large enhancement in the SERS signal of the *P. aeruginosa* after releasing the stress. The baseline-corrected peak height of the SERS of *P. aeruginosa* located at about 1323 cm^{-1} was used to quantify the overall SERS response and was chosen to calculate the increment in the SERS signal, f , as:

$$f = \frac{I_{\text{released}} - I_{\text{background}}}{I_{\text{stretched}} - I_{\text{background}}} \quad (1)$$

where I_{released} and $I_{\text{stretched}}$ are the Raman intensities of 1323 cm^{-1} peak on relaxed and pre-stretched AgNR-PDMS substrates, $I_{\text{background}}$ is the background intensity of the spectra. The Raman spectra of *P. aeruginosa* on stretched AgNR-PDMS substrate was used as reference.

Interestingly, it can be noticed that the AgNRs-PDMS substrate offers an almost eleven times higher Raman signal compared to pre-stretched AgNR-PDMS substrate. The increase in Raman signal after releasing the strain may be attributed to two factors. One is the better attachment and second is the increased number of hotspots. The buckled AgNR-PDMS substrate provides cage like structure to capture *P. aeruginosa* by AgNRs from the bottom surface as well as from sides. The AgNRs deposited over stretched elastomeric PDMS films were subjected to initial mechanical strain (ϵ), upon releasing the strain periodic wrinkles were formed to minimize the strain energy. The periodicity (λ) and the amplitude (A) of these wrinkles were simply tuned by varying the strain values (ϵ) and has been studied in detail elsewhere.⁴⁰ The periodicity (λ) for the wrinkled Ag nanorods arrays on PDMS is found to be about 3.5 μm for 30% strain value. The magnified view of the corresponding wrinkled AgNRs arrays on PDMS are shown in Figure S1(c), ESI. Deposition of AgNRs film on a pre-stretched PDMS substrate provides a big difference in elastic moduli at the interface of the film and results into the formation of wrinkles on releasing

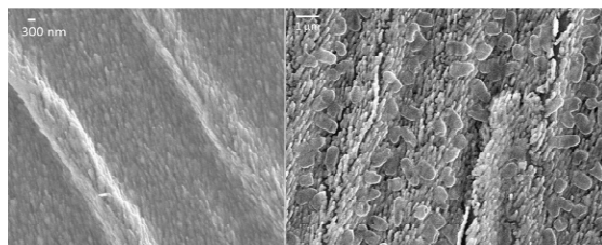
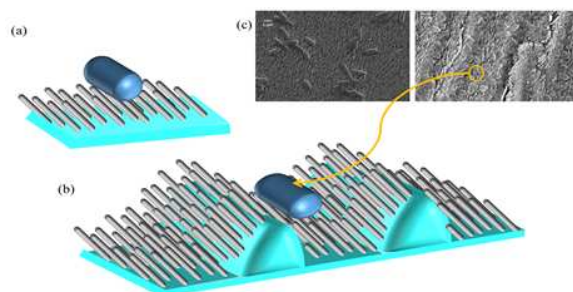


Figure 2. (a) Wrinkled AgNR-PDMS after releasing strain. (b) Aligned *P. aeruginosa* along the grooves of wrinkled AgNR-PDMS.

the strain. These wrinkled AgNR-PDMS substrate provides a cage like structure to capture *P. aeruginosa*. When bacteria is on a pre-stretched AgNR-PDMS substrate only the nanorods under the bacteria are in contact with it. After the strain is released, the periodic grooves form and *P. aeruginosa* bacteria become aligned parallel to the groove axis as seen in figure 2. The formation of grooves increases the total contact area of the nanorods to the bacteria and hence, increases the number of active SERS spots resulting into a comparatively higher Raman Signal (Scheme 2).

Another factor that may contribute to the enhanced Raman signal is the number of hotspots. The Average number density of AgNR increases slightly from 8.5×10^8 NR/cm² to 11.2×10^8 NR/cm² after releasing the strain. The increase in the number of nanorods is small around 30% that may have a slight contribution. For cyclic measurements the stress-release cycle was repeatedly applied (Fig. S3, ESI[†]). The pre-stretched AgNR-PDMS substrate was cycled back and forth between stretched and relaxed position and SERS spectra was acquired after each stretching and relaxed state. The Raman intensity decreases for second and third cycle with respect to the first cycle. The decrease in the increment factor f after first cycle may be attributed to the damage in the AgNR-PDMS substrate on successive release and stretching of the substrate. The increment factor f after each cycle was calculated by taking the intensity ratio of the 1323 cm^{-1} peak before and after each cycle. It may also decrease because the SERS intensity observed in stretched position, after second stretch cycle was always higher than that on



Scheme 2. Schematic showing *P. aeruginosa* on (a) prestretched and (b) wrinkled AgNR-PDMS substrate (c) SEM of *P. aeruginosa* on prestretched and wrinkled AgNR-PDMS substrate

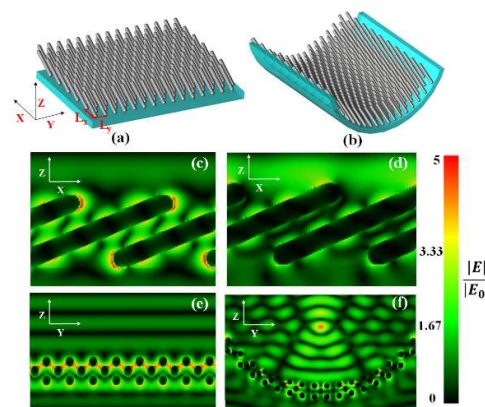


Figure 3. Geometries used in FDTD simulation with the variation of electric field on and above the silver nanorods. ($|E|/|E_0|$ is the local field enhancement) (a) Simulation geometry for flat substrate. (b) Simulation geometry for buckled substrate modeled as a curved surface. (c) X-Z slice of field on the nanorods for flat geometry. (d) X-Z slice of field on the nanorods for curved geometry. (e) Y-Z slice of field on and above the nanorods for flat geometry. (f) Y-Z slice of field on and above the nanorods for curved geometry.

the pristine pre-stretched AgNRs-PDMS substrate and hence, the Raman signal decreases but still it is higher than the pre-stretched AgNR-PDMS substrate. Another reason may be that during the stretching and releasing, the shape of the bacteria may change, and some parts of the bacteria may be attached to the AgNRs. In this process, due to nanocarpenter effect, nanorods may be bundled by the capillary force to form clusters.⁴¹ This effect alters the structural formation and morphology of the nanorod arrays which may be one of the reason behind the decrease in Raman Intensity. The detection limit obtained was approximately 1×10^4 CFU/ml.

In order to investigate the local field enhancement on the flat and buckled PDMS Substrates, the finite difference time domain (FDTD) numerical simulations were carried out. Fig. (3) (a) and (b) are showing the modeled geometries for flat and buckled substrates respectively, see the Supporting Information S1 for details. The incident laser beam of wave length 514 nm was used as external excitation. Fig. (c) and (d) are showing cross sectional view of local field enhancement on the surface of nanorods for flat and curved substrates. It has been shown that the local field enhancement on the nanorods surfaces of flat and curved substrates are not so much of difference. But in case of curved geometry as seen in figure (f) there is a formation of central spot with higher electric field value, this is the place where bacteria's are caged in the buckled geometry. This spot is not forming in case of flat geometry fig. (e). In case of buckled substrate the number of nanorods which are touching the bacteria's surface are large because of caging and higher density of nanorods.

To show the degree of reproducibility of the preparation and spectroscopic measurements the spectra of two different samples of *P. aeruginosa* (prepared and measured at different dates), Fig. S4, ESI. We see that the differences between the two spectra appear to be rather small, though one cannot entirely rule out that

some secondary differences are present. Although the spectra in Fig. S4, ESI are similar and the reproducibility is good, there are some differences in the major bands in the region 1300-1500 cm^{-1} . This region can be expected to involve the groups that have the strongest interaction with the silver surface. It is likely that slight variations in the parameters such as the concentration of bacteria, and the time of adsorption affect this interaction and alter the spectrum. To demonstrate the potential application of the buckled AgNRs-PDMS as a SERS substrate *Bacillus* and *E. coli* were also studied under similar set of conditions. The details can be found in the Fig. S6, ESI. The SERS signals of these two bacteria were also found to increase around ten times on releasing the strain. In conclusion, we have successfully demonstrated a simple and facile method to increase the SERS enhancement of bacteria due to the formation of high density hot spots among the AgNRs and the increase in the area for better interaction of bacteria to the metal surface. This AgNRs-PDMS buckled system provides the better entrapment and increased contact area of the *P. aeruginosa* onto the AgNRs giving rise to enhancement in the Raman signal.

Notes and references

- 1 F. Ratjen and G. Döring, *Lancet*, 2003, 361, 681–9.
- 2 M. Robinson and P. T. B. Bye, *Pediatr. Pulmonol.*, 2002, 33, 293–306.
- 3 E. Sadeghi, A. Matlow, I. MacLusky and M. A. Karmali, *J. Clin. Microbiol.*, 1994, 32, 54–8.
- 4 F. Bittar, H. Richet, J.-C. Dubus, M. Reynaud-Gaubert, N. Stremmler, J. Sarles, D. Raoult and J.-M. Rolain, *PLoS One*, 2008, 3, e2908.
- 5 A. Sengupta, M. Mujacic and E. J. Davis, *Anal. Bioanal. Chem.*, 2006, 386, 1379–86.
- 6 C. Fang, A. Agarwal, K. D. Buddharaju, N. M. Khalid, S. M. Salim, E. Widjaja, M. V. Garland, N. Balasubramanian and D.-L. Kwong, *Biosens. Bioelectron.*, 2008, 24, 216–21.
- 7 K. Kneipp, H. Kneipp, V. B. Kartha, R. Manoharan, G. Deinum, I. Itzkan, R. R. Dasari and M. S. Feld, *Phys. Rev. E*, 1998, 57, R6281–R6284.
- 8 X. Wang, W. Hao, H. Zhang, Y. Pan, Y. Kang, X. Zhang, M. Zou, P. Tong and Y. Du, *Spectrochim. Acta. A. Mol. Biomol. Spectrosc.*, 2015, 139, 214–21.
- 9 R. M. Jarvis and R. Goodacre, *Chem. Soc. Rev.*, 2008, 37, 931–6.
- 10 J. Chen, G. Qin, W. Shen, Y. Li and B. Das, *J. Mater. Chem. C*, 2015, 3, 1309–1318.
- 11 J. Chen, G. Qin, J. Wang, J. Yu, B. Shen, S. Li, Y. Ren, L. Zuo, W. Shen and B. Das, *Biosens. Bioelectron.*, 2013, 44, 191–197.
- 12 D. L. Jeanmaire and R. P. Van Duyne, *J. Electroanal. Chem. Interfacial Electrochem.*, 1977, 84, 1–20.
- 13 M. Moskovits, *Rev. Mod. Phys.*, 1985, 57, 783.
- 14 G. Rusciano, P. Capriglione, G. Pesce, P. Abete, V. Carnovale and A. Sasso, *Laser Phys. Lett.*, 2013, 10, 075603.
- 15 X. Wu, J. Chen, X. Li, Y. Zhao and S. M. Zughaier, *Nanomedicine*, 2014, 10, 1863–70.
- 16 M. Suzuki, W. Maekita, Y. Wada, K. Nakajima, K. Kimura, T. Fukuoka and Y. Mori, *Appl. Phys. Lett.*, 2006, 88, 203121.
- 17 F. Bayata, Z. B. Akinci, A. S. Donatan and M. Urgen, *Mater. Lett.*, 2012, 67, 387–389.
- 18 S. Kumar, P. Goel, D. P. Singh and J. P. Singh, *Appl. Phys. Lett.*, 2014, 104, 023107.
- 19 G. Lu, H. Li and H. Zhang, *Chem. Commun.*, 2011, 47, 8560–8562.
- 20 G. Lu, H. Li and H. Zhang, *Small*, 2012, 8, 1336–1340.
- 21 J. P. Singh, H. Chu, J. Abell, R. A. Tripp and Y. Zhao, *Nanoscale*, 2012, 4, 3410–4.
- 22 C. Qian, C. Ni, W. Yu, W. Wu, H. Mao, Y. Wang and J. Xu, *Small*, 2011, 7, 1800.
- 23 E.-Z. Tan, P.-G. Yin, T.-T. You, H. Wang and L. Guo, *ACS Appl. Mater. Interfaces*, 2012, 4, 3432–7.
- 24 S. C. Xu, Y. X. Zhang, Y. Y. Luo, S. Wang, H. L. Ding, J. M. Xu and G. H. Li, *Analyst*, 2013, 138, 4519–25.
- 25 K. A. Stoerzinger, J. Y. Lin and T. W. Odom, *Chem. Sci.*, 2011, 2, 1435–1439.
- 26 Q. Zhang, Y. H. Lee, I. Y. Phang, C. K. Lee and X. Y. Ling, *Small*, 2014, 10, 2703–11.
- 27 M. Yilmaz, E. Senlik, E. Biskin, M. S. Yavuz, U. Tamer and G. Demirel, *Phys. Chem. Chem. Phys.*, 2014, 16, 5563–70.
- 28 Y. Zhao, D. Ye, G.-C. Wang and T.-M. Lu, *Opt. Sci. Technol. SPIE's 48th Annu. Meet.*, 2003, 5219, 59–73.
- 29 K. Robbie, *J. Vac. Sci. Technol. B Microelectron. Nanom. Struct.*, 1998, 16, 1115.
- 30 C. S. and M. L. and Y. M. and A. B. and C. K. and P. J. S. B. and T. A. S. and A. L. and M. Köller, C. Sengstock, M. Lopian, Y. Motemani, A. Borgmann, C. Khare, P. J. S. Buenconsejo, T. A. Schildhauer, A. Ludwig and M. Köller, *Nanotechnology*, 2014, 25, 195101.
- 31 W. R. Premasiri, Y. Gebregziabher and L. D. Ziegler, *Appl. Spectrosc.*, 2011, 65, 493–9.
- 32 I-Fang Cheng, H.-C. Chang, T.-Y. Chen, C. Hu, F.-L. Yang, I.-F. Cheng, H.-C. Chang, T.-Y. Chen, C. Hu and F.-L. Yang, *Sci. Rep.*, 2013, 3, 2365.
- 33 C. Sandt, T. Smith-Palmer, J. Pink and D. Pink, *Appl. Spectrosc.*, 2008, 62, 975–983.
- 34 J. De Gelder, K. De Gussem, P. Vandenabeele and L. Moens, *J. Raman Spectrosc.*, 2007, 38, 1133–1147.
- 35 J. M. Benevides, S. A. Overman and G. J. Thomas, *Current protocols in protein*, John Wiley & Sons, Inc., Hoboken, NJ, USA, 2001, Chapter 17, p. Unit 17.8.
- 36 F. S. de Siqueira e Oliveira, H. E. Giana and L. Silveira, *J. Biomed. Opt.*, 2012, 17, 107004.
- 37 L. Zeiri and S. Efrima, *J. Raman Spectrosc.*, 2005, 36, 667–675.
- 38 E. C. López-Díez, C. L. Winder, L. Ashton, F. Currie and R. Goodacre, *Anal. Chem.*, 2005, 77, 2901–6.
- 39 K. Hamasha, Q. I. Mohaidat, R. A. Putnam, R. C. Woodman, S. Palchadhuri and S. J. Rehse, *Biomed. Opt. Express*, 2013, 4, 481–489.
- 40 P. Goel, S. Kumar, J. Sarkar and J. P. Singh, *ACS Appl. Mater. Interfaces*, 2015, 7, 8419–8426.
- 41 J.-G. Fan, D. Dyer, G. Zhang and Y.-P. Zhao, *Nano Lett.*, 2004, 4, 2133–2138.